

# Geophysical Research Letters

## RESEARCH LETTER

10.1029/2020GL088773

### Key Points:

- Wind and sediment flux decrease downwind from the leading edge of White Sands Dune Field
- A Lagrangian 1-D model explains how nonequilibrium flow induced by surface roughness transitions produces observed dynamics
- Results are generalized using the 1-D model for other roughness scenarios

### Supporting Information:

- Supporting Information S1
- Figure S1
- Figure S2
- Figure S3
- Figure S4
- Figure S5

### Correspondence to:

D. J. Jerolmack,  
sediment@sas.upenn.edu

### Citation:

Gunn, A., Schmutz, P., Wanker, M., Edmonds, D. A., Ewing, R. C., & Jerolmack, D. J. (2020). Macroscopic flow disequilibrium over aeolian dune fields. *Geophysical Research Letters*, 47, e2020GL088773. <https://doi.org/10.1029/2020GL088773>

Received 7 MAY 2020

Accepted 24 JUL 2020

Accepted article online 6 AUG 2020

### Author Contributions

**Conceptualization:** A. Gunn,

D. A. Edmonds, R. C. Ewing,

D. J. Jerolmack

**Data curation:** A. Gunn, P. Schmutz,

M. Wanker, D. A. Edmonds,

R. C. Ewing, D. J. Jerolmack

**Methodology:** A. Gunn, P. Schmutz,

M. Wanker, D. A. Edmonds,

R. C. Ewing, D. J. Jerolmack

**Software:** A. Gunn

**Validation:** A. Gunn

**Writing - Original Draft:** A. Gunn

**Formal Analysis:** A. Gunn

**Investigation:** A. Gunn, P. Schmutz,

M. Wanker, D. A. Edmonds,






R. C. Ewing, D. J. Jerolmack

**Project Administration:**

D. A. Edmonds, R. C. Ewing,

D. J. Jerolmack

## Macroscopic Flow Disequilibrium Over Aeolian Dune Fields

A. Gunn<sup>1</sup> , P. Schmutz<sup>2</sup> , M. Wanker<sup>3</sup>, D. A. Edmonds<sup>3</sup> , R. C. Ewing<sup>4</sup> ,  
and D. J. Jerolmack<sup>1,5</sup> 

<sup>1</sup>Department of Earth and Environmental Science, University of Pennsylvania, Philadelphia, PA, USA, <sup>2</sup>Department of Earth and Environmental Science, University of West Florida, Pensacola, FL, USA, <sup>3</sup>Department of Earth and Atmospheric Sciences, Indiana University, Bloomington, IN, USA, <sup>4</sup>Department of Geology and Geophysics, Texas A&M University, College Station, TX, USA, <sup>5</sup>Department of Mechanical Engineering and Applied Mechanics, University of Pennsylvania, Philadelphia, PA, USA

**Abstract** Aeolian dune fields are self-organized patterns formed by wind-blown sand. Dunes are topographic roughness elements that impose drag on the atmospheric boundary layer (ABL), creating a natural coupling between form and flow. While the steady-state influence of drag on the ABL is well studied, nonequilibrium effects due to roughness transitions are less understood. Here we examine the large-scale coupling between the ABL and an entire dune field. Field observations at White Sands, New Mexico, reveal a concomitant decline in wind speed and sand flux downwind of the transition from smooth playa to rough dunes at the upwind dune-field margin, that affects the entire ~10-km-long dune field. Using a theory for the system that accounts for the observations, we generalize to other roughness scenarios. We find that, via transitional ABL dynamics, aeolian sediment aggradation can be influenced by roughness both inside and outside dune fields.

**Plain Language Summary** Just as how cyclists opt to have smooth skin to gain a speed advantage, near-surface winds in the atmosphere are faster over smooth topography. Dunes slow winds down because they are rough, but these features are also shaped by the winds. When wind passes over a boundary between smooth and rough surfaces, it cannot instantaneously slow down; instead, there is a transition zone where it decelerates. This area of transition can exist at the edge of a dune field if the land upwind of it is relatively smooth. We observe this at White Sands Dune Field, and generalize the results with theory. Aside from helping to explain the striking patterns we see on planetary surfaces, this result is useful because dunes are often used to interpret wind conditions.

## 1. Introduction

Aeolian dune fields are patterned areas of sand that express an aerodynamic coupling between the Earth's erodible surface and the atmospheric boundary layer (ABL) (Bagnold, 1941; Kocurek & Ewing, 2005). For a single dune, this coupling is clear: flow accelerates on the stoss which erodes sand, and sand deposits on the lee where flow separates (Pye & Tsoar, 2008). For a pair of dunes, the flow wake generated by an upwind dune influences the flow over a dune downwind, creating short-range interaction (Bacik et al., 2020; Bristow et al., 2019). For many dunes, the sum of their wakes imparts a collective drag (Stevens et al., 2015), creating a roughness sublayer in the ABL a few dune-heights high (Ghisalberti, 2009). When there is a separation of scales between the bodies and the flow, we parameterize this many-body effect on the ABL inertial layer aloft with a roughness length  $z_0$  (Nield et al., 2013; Nikuradse, 1950; Stull, 2012). This is done extensively for dune-sized bodies in the ABL when flow is in equilibrium with the surface below (Garratt, 1990). Dune fields have edges, however, and the mismatch of roughness imparted by the dunes and the external surface can lead to a breakdown of equilibrium conditions downwind of the edge. This transient phenomena is rarely studied in geomorphology, with a few exceptions (Bauer, 1991; Jerolmack et al., 2012).

In the field of boundary layer meteorology, however, there has been significant work on how ABL flow changes due to a Lagrangian transition in surface properties; be it heat, water vapor flux, or roughness (Bou-Zeid et al., 2004; Dupont & Brunet, 2009; Garratt, 1990). Observations, empirical relations, and numerical models all describe a common pattern: When flow meets an edge between two surfaces, there is some

**Resources:** A. Gunn, D. A. Edmonds, R. C. Ewing, D. J. Jerolmack  
**Supervision:** D. J. Jerolmack  
**Visualization:** A. Gunn  
**Writing - review & editing:** A. Gunn, D. A. Edmonds, R. C. Ewing, D. J. Jerolmack

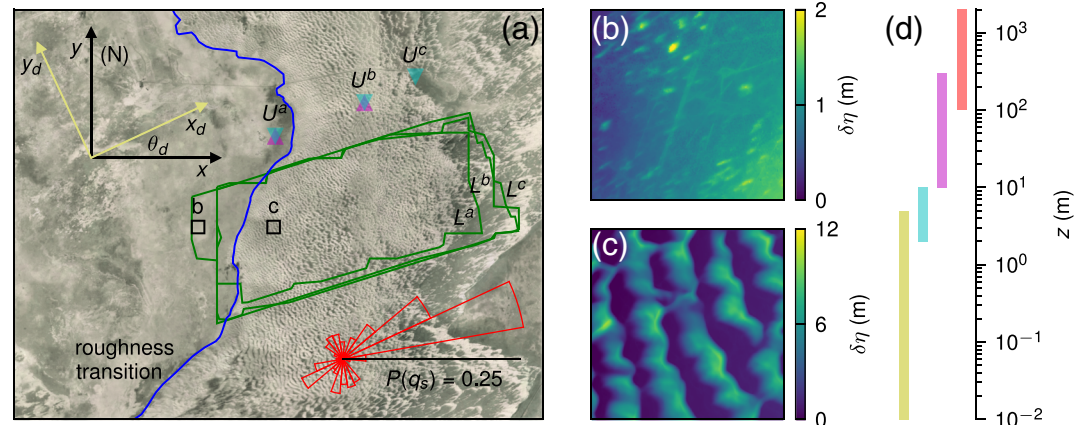


**Figure 1.** (a) A composite aerial photograph of White Sands Dune Field, New Mexico, annotated with three topographic lidar data set boundaries in green ( $L^a$ ,  $L^b$ ,  $L^c$ ), three ABL measurement locations ( $U^a$ ,  $U^b$ , and  $U^c$ ) for meteorological towers (cyan arrows) and Doppler lidar (magenta arrows), the roughness transition delineating the “smooth” playa and dune field (blue line), two pairs of axes  $[x, y]$  (black, cardinal) and  $[x_d, y_d]$  (yellow) that are offset by the dune direction  $\theta_d$ . Axes lines are 5 km centered on  $[32.854^\circ, -106.369^\circ]$ . A sediment flux probability rose calculated from the tower at  $U^a$  (red), black line gives scale. (b, c) 500 m<sup>2</sup> sub-DTMs (locations in black in panel a) contrast playa and dune topography (note the different color-scales of elevation relative to sub-DTM minimum,  $\delta\eta$ ). (d) The approximate range of elevations for dune field topography (yellow), meteorological tower observations (cyan), wind lidar (magenta), and ABL height (red).

transient disequilibrium between flow and the surface downwind of the edge. While this work has many valuable applications, in urban weather and renewable energy, for example (Barlow, 2014; Stevens et al., 2015), none of these efforts have focused on flow crossing a dune field boundary. This is a notable case, however, since the flow creates the form, which in turn alters the flow.

Jerolmack et al. (2012) presented the idea of an internal boundary layer developing over the White Sands Dune Field in New Mexico, USA. This dune field has a unidirectional sediment flux (Figures 1a and S1 in the supporting information) and a well-defined dune field boundary, where a consistently “smooth” upwind playa transitions to active “rough” dunes (Kocurek et al., 2007; McKee, 1966). Jerolmack et al. (2012) hypothesized that the transition creates flow deceleration across the dune field, causing measured changes in dune migration that control vegetation density and even the groundwater table. They did not make direct wind observations, however; in lieu of this, Jerolmack et al. (2012) drew upon empirical closures from classical boundary layer studies that seldom apply to the ABL. Furthermore, since their study, alternative hypotheses for the observed dune migration patterns at White Sands have arisen that dispute the influence of the roughness transition (Baitis et al., 2014; Pelletier, 2015). To resolve this conflict, we apply a recent transient ABL theory (Momen & Bou-Zeid, 2016) to White Sands, finding the wind adjustment due to roughness change and the associated lengthscale. We then present measurements of winds and topography at White Sands (Figure 1) that agree with the theoretical prediction. We examine near-surface winds at three locations on a streamwise transect, winds up to 300 m at two locations (Gunn et al., 2018), and dune migration patterns from three topographic surveys. Our work shows that at White Sands the ABL is out-of-equilibrium with the dune roughness creating streamwise gradients in sediment flux. Finally, with theory we suggest that this mechanism is significant for most dune fields on Earth.

## 2. Materials and Methods

### 2.1. ABL Theory

We first seek to develop a physically informed expectation of the flow adjustment at the leading edge of a dune field. Models of the ABL cover a broad range of complexity. Often, computationally expensive large eddy simulations (LES) are chosen to understand the temporal response of the ABL to forcing. The richness of each LES experiment, however, comes at the expense of limiting the number of forcings examined. Instead, we chose to employ an analytical model extending from Momen and Bou-Zeid (2016), opting for the ability to generalize and interpret. Such a model seems appropriate also given the limited data available for comparison.

The main assumption of this model is that the turbulent stresses responsible for mixing momentum vertically in the ABL are linearly proportional to the local horizontal flow speed. Using a Reynolds decomposition where  $u = \bar{u} + u'$ ,

$$\frac{\partial(u'w')}{\partial z} \simeq \alpha \bar{u}. \quad (1)$$

Here  $u$  is horizontal wind speed,  $w$  is vertical wind speed,  $z$  is altitude, and  $\alpha$  is a damping frequency that is proportional to how easily momentum is transferred. An identical equation is assumed for the orthogonal horizontal wind speed  $v$ . We further assume that the ABL is neutral, barotropic, and locally planar-homogeneous. Then, if we let  $A = u + iv$ , where  $i$  is the imaginary unit and set the geostrophic wind vector to  $A_g = G + i \cdot 0$ , the ABL flow equation is

$$\dot{A} = if(G - A) - \alpha A, \quad (2)$$

where the over-dot indicates change in time and  $f$  is the Coriolis frequency. Steady-state flow therefore takes the form  $A = G/(1 - i\alpha/f)$ .

Now consider the case where a Lagrangian column of air that is in equilibrium,  $A_{out}$ , encounters a step change in environment characterized by  $\alpha_{in}$  at  $t = 0$  such that it tends toward a new equilibrium  $A_{in}$ ; the solution to Equation 2 is

$$A = \underbrace{x A_{out}}_{\text{homogeneous}} + \underbrace{(1 - x) A_{in}}_{\text{particular}}, \quad (3)$$

where  $x = e^{-t(\alpha_{in} + if)}$ . Assuming Taylor's hypothesis, we can switch from a Lagrangian reference frame to an Eulerian one. A parcel in the column travels with the flow  $U$  where  $U = |A|$ , such that  $t = S/U$  where  $S$  is the streamwise distance from the step change in environment.

Using Equation 3 in an Eulerian reference frame, we can describe the transience that is caused by flow encountering a change in roughness between the inside and outside of a dune field—all that is required is a model that links momentum with roughness via  $\alpha$ . Here we choose the following model used by others (Herrmann & Madsen, 2007; Lentz, 2001; Momen & Bou-Zeid, 2016):

$$\alpha = \frac{A_g L_0}{\log(z/z_0) Z^2} \quad (4)$$

where there are three characteristic lengthscales:  $L_0$  for turbulent mixing,  $z_0$  for roughness, and  $Z$  for ABL height. To apply Equations 3 and 4, we choose values for the free parameters  $L_0$ ,  $Z$ ,  $z_{0,out}$ ,  $z_{0,in}$ , and  $f$ . Following verification from LES (Momen & Bou-Zeid, 2016) we choose  $L_0 = 50$  m. At White Sands the average ABL height is approximately  $Z = 1,000$  m (Hinds & Hoidale, 1977) (red line Figure 1d), and the latitude constrains  $f = 7.91 \cdot 10^{-5} \text{ s}^{-1}$ . We assume  $z_{0,out} = 10^{-4}$  m for the playa and  $z_{0,in} = 10^{-1}$  m for the dune field. These follow typical values for boundary layer studies of similar landscapes (Stull, 2012), and the classical result from hydraulically rough flow where  $z_0 = k_s/30$  and  $k_s$  is the element height (a ripple and a dune for upwind and downwind, respectively, Figure 1d) (Nikuradse, 1950). With these elements in place, we are able to predict the magnitude and distance of the expected downwind decrease in wind speed at White Sands.

## 2.2. ABL Observations

We observed the winds at White Sands Dune Field using two separate systems: a set of three 10-m meteorological towers measuring near-surface concurrently, and a single upward facing Doppler wind lidar measuring wind profiles at heights  $10 \text{ m} \leq z \leq 300 \text{ m}$  at two separate locations on consecutive years. The periods of observation for all instruments overlapped with the “windy season,” in which strong southwesterly winds emanating from the Pacific cross New Mexico between February and June (Hinds & Hoidale, 1977).

The three meteorological towers were erected in 2015 along a transect approximately in the “formative” wind direction (cyan triangles at  $U^a$ ,  $U^b$ , and  $U^c$  in Figure 1a, respectively). These towers measured wind speeds at 2, 5, and 10 m elevation, and wind direction at 10 m elevation, using cup and vein anemometers (cyan line Figure 1d). Data were stored for the 10-min means. The harsh environment at White Sands Dune Field (heat waves, dust storms, lightning, etc.) has limited when these towers were able to measure all variables concurrently, to 160 days. Only these periods are reported here.

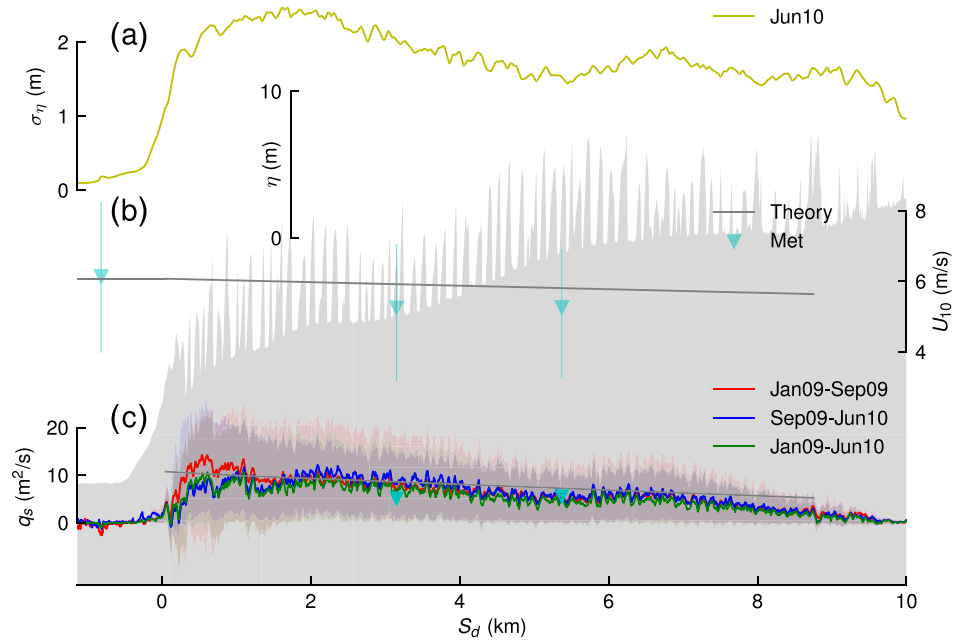


**Figure 2.** White Sands transects in  $S_d$ , the streamwise direction where the roughness transition is at the origin. Bumpy shaded background is an example DTM elevation,  $\eta$ , transect illustrating the roughness transition and net deposition. (a) The spanwise mean local topographic standard deviation (yellow line),  $\sigma_\eta$ , shown here for the June 2010 DTM, is low upwind of the margin and consistently high downwind. This causes a deceleration in 10-m wind,  $U_{10}$ , shown for theory (upper gray line) and concurrent observations (cyan; triangles, average; lines, interquartile range) in (b). In turn, (c) the sediment flux,  $q_s$ , diminishes downwind, as measured explicitly from DTM pairs (red, blue, and green; lines, spanwise average; envelopes, spanwise interquartile range) and calculated from theory (lower gray line) and dune-aligned 10-m winds (cyan triangles). Sediment flux calculated with  $U_{10}^a$  is not shown due to limited sediment supply on the playa.

A Zephir300 lidar recorded data adjacent to Tower A for 59 days in 2016, and to Tower B for 18 days in 2017 and was used to measure the winds between 10 and 300 m elevation (magenta triangles at  $U^a$  and  $U^b$  in Figure 1a, respectively). Means for 17-s intervals at 10 elevations between 10 and 300 m (magenta line Figure 1d) were taken. Here we only report the horizontal wind speeds.

### 2.3. Topography Observations

We analyze three White Sands Dune Field terrestrial airborne lidar survey DTMs to understand the dune direction and sediment fluxes. These surveys are publicly available on OpenTopography.org and were taken in January 2009, September 2009, and June 2010 ( $L^a$ ,  $L^b$ , and  $L^c$  in Figure 1a, respectively). Dune direction, that is, the direction a dune migrates,  $\theta_d$ , was found by analyzing the slip-face orientations (Pedersen et al., 2015; Swanson et al., 2016) using a cross-correlation technique (Text S1 and Figure S1 in the supporting information). Sediment flux,  $q_s$ , was found by integrating the Exner equation,

$$q_s(s) = q_s(s_0) - \phi \int_{s_0}^s \frac{d\eta}{dt} dx_d, \quad (5)$$

where  $\phi$  is the packing fraction,  $s$  is some distance along a line of constant  $y_d$ ,  $d\eta$  is a change in elevation over some time interval  $dt$ , and  $q_s(s)$  is the sediment flux  $q_s$  at some location  $s$ . If  $q_s(s_0)$  is known, then  $q_s(s)$  can be found by performing the integral on the RHS of Equation 5 (Text S1 and Figures S2 and S3).

## 3. Results

The impact of the roughness transition can be seen in both form and flow at White Sands (Figure 2). To illustrate the difference in topographic variability that induces flow drag, we plot the spanwise average transect in standard deviation over a  $100 \text{ m}^2$  moving window (yellow line). The playa outside the dune field,  $S_d < 0$ , is smooth relative to the dunes, which can also be seen in an example elevation transect (gray background in Figure 2). Average downwind flow deceleration in 10-m wind is shown for concurrent Met tower



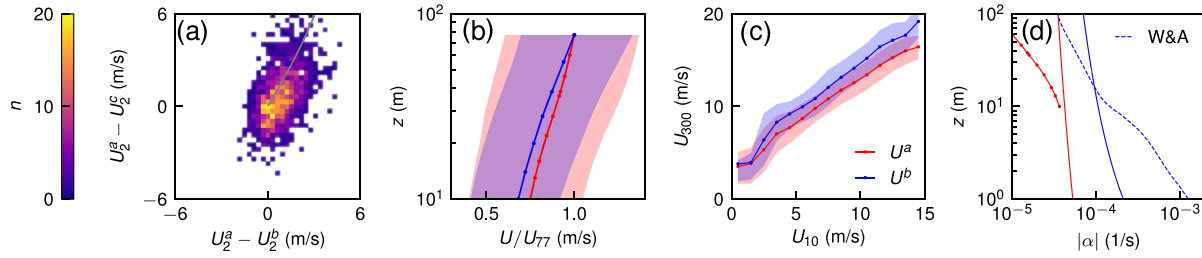


**Figure 3.** (a) A histogram of residuals between concurrent 2-m wind speeds,  $U_2^a$ ,  $U_2^b$ , and  $U_2^c$ , at the three meteorological towers, with theory (gray line) overlaid. (b) Mean Doppler lidar wind speed profiles between 10 and 77 m (for  $\theta_{10} \in \{\theta_d \pm 15^\circ\}$ ) from the playa ( $U^a$ , red line) and within the dune field ( $U^b$ , blue line), normalized and plotted with interquartile range envelopes. (c) Mean (lines) and interquartile ranges (envelopes) of  $U_{300}$  given  $U_{10}$ . (d) Theoretical profiles of the damping frequency,  $\alpha$ , for the playa (red) and the dune field (blue) for a fixed geostrophic condition, and inferred profiles from the playa Doppler lidar (red dotted line) and LES simulations by Wang and Anderson (2019) (blue dashed line).

measurements (cyan in Figure 2b). These speeds are filtered such that for a given time, wind direction is within  $\theta_d \pm n \cdot 15^\circ$  where  $n = \{1, 2, 3\}$  for  $U_a$ ,  $U_b$ , and  $U_c$ , respectively, meaning flow is approximately aligned with the dunes everywhere. The idealized model (gray line in Figure 2b) gives fair agreement with the observed deceleration. This theory line is the weighted average of an ensemble of lines with different  $G$  values such that it has the same observed probability of  $U_{10}^a$  values. This averaging is important because flow deceleration is nonlinearly related to the upwind speed (Equation 2). The coupling between flow and form is then closed by sediment flux, which we illustrate in three independent calculations (Figure 2c). Explicit measurement of sediment flux comes from DTM pairs, which show transport diminishing downwind. We compare this to sediment flux calculations determined from measured  $U_{10}$  winds at Met towers  $U^b$  and  $U^c$  (for  $\theta \in \{\theta_d \pm 15^\circ\}$ ), using the following relations linking  $U_{10}$  and  $q_s$ :

$$U_{10} = \frac{u_*}{\kappa} \log \left( \frac{10}{z_0} \right), \quad (6)$$

$$q_s = K_q \frac{\rho_{air}}{g \rho_{sand}} u_{*,cr} \left( u_*^2 - u_{*,cr}^2 \right),$$

where  $u_*$  is the friction velocity,  $\kappa$  is von Karman's constant,  $\rho$  is the density of the subscripts,  $g$  is gravity, and  $u_{*,cr}$  is the critical friction velocity above which sediment transport is initiated. Equation 6 has been used elsewhere (Durán et al., 2011; Kok et al., 2012), and here  $K_q = 2.87$  is inferred mean value of two experimental studies (Ho et al., 2011; Li et al., 2010). Our choice of  $u_{*,cr} = 0.3$  m/s is within the range previously used at White Sands (Eastwood et al., 2012; Jerolmack et al., 2011; Reitz et al., 2010);  $z_0$  used in this flux calculation is  $10^{-4}$  m, since wind at the saltation scale “feels” the ripple-scale drag, consistent with other studies from White Sands (Gunn et al., 2018; Jerolmack et al., 2006; Martin et al., 2013). The chosen parameter values predict a flux decline that reasonably follows the DTM-derived trend, while parameterizing roughness as  $z_0 \sim \sigma_\eta(S_d)$ , following previous work (Anderson et al., 2012; Garratt, 1994; Shockling et al., 2006), measured with the DTM marginally improves the prediction (Text S2 and Figure S4).

The roughness transition at White Sands also affects ABL flow structure (Figure 3). To show the downwind evolution of near-surface wind, residuals of aligned concurrent wind speeds measured by the towers are plotted in Figure 3a. Consistent with theory, observations prefer the NNE octant of this space such that  $U_2^a > U_2^b > U_2^c$ . The magnitudes of these residuals are large enough to indicate that sediment flux sometimes occurs at upwind locations, but not downwind, in the dune field. Doppler lidar flow profiles far above the dunes are also altered substantially for dune-aligned winds, such that for a given speed aloft the near-surface shear is diminished inside the dune field relative to outside (Figure 3b). In turn, this ensures that flow aloft must be greater over the dune field to achieve the same near-surface speed, with this compensation growing with magnitude (Figure 3c). The damping frequency  $\alpha$  parameterizes how much shear-induced turbulent mixing there is given mean flow speed (Equation 1). Theoretical profiles of  $\alpha$  consistent with (Momen & Bou-Zeid, 2016, 2017) for the constants at White Sands and  $G = 20$  m/s (Jerolmack et al., 2012) are compared to profiles inferred from assumed-equilibrium flows in Figure 3d. The inferred  $\alpha$  profiles are found using wind profiles and rearranging Equation 3 with  $\dot{A} = 0$ . This assumption, that flow is locally steady, should hold for the average profile measured by the Doppler wind lidar at  $U^a$ , and a LES simulation over a periodic subdomain of White Sands dunes performed by Wang and Anderson (2019). The lidar and LES should be compared to the theoretical profiles outside and inside the dune field, respectively. They

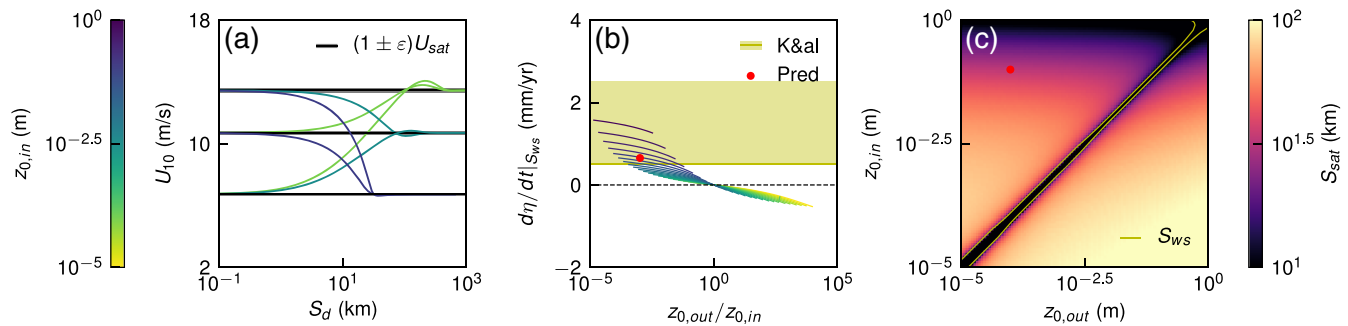


**Figure 4.** (a) Theoretical scenarios of the evolution of 10-m wind speed ( $U_{10}$ ) with distance downwind ( $S_d$ ) of a transition from roughness lengths of  $z_{0,out}$  to  $z_{0,in}$ . Line color indicates  $z_{0,in}$  from the left color bar, and black lines indicate equilibrium speeds,  $U_{sat}$  (small gray envelopes are within 1% of  $U_{sat}$ ). (b) Theoretical deposition rates,  $d\eta/dt$ , at distance  $S_{ws}$  downwind of the transition for a given ratio of outside and inside (line color)  $z_0$ . Overlaid is the prediction for White Sands (red dot) and measured deposition rate (yellow; line, present day; envelope, interquartile range over last  $\sim 7.3$  ka) using OSL dating by Kocurek et al. (2007). (c) The theoretical distance  $S_{sat}$  downwind of a roughness transition to achieve  $U_{10}$  that is in equilibrium with  $z_{0,in}$ , where color has a log scale. Streamwise length of White Sands Dune Field at the measured wind transect is  $S_{ws} = 5$  km (yellow line); and the assumed White Sands  $z_{0,out}$  and  $z_{0,in}$  (red dot) are shown.

show that the parameterization for  $\alpha$  in Equation 4 underestimates the vertical gradient in damping but is consistent at 10 m, where the ABL theory is tied to sediment flux with Equation 6 (Text S2 and Figure S4).

The results from White Sands indicate that the roughness disparity at the dune field boundary has geomorphic consequences. This could occur in dune fields with different dune and external roughness lengths. We broaden our results by varying roughness lengths inside and outside a hypothetical region in the idealized theory with  $G = 20$  m/s (Figure 4). This exercise approximates the isolated coupling of flow and the erodible form that impinges upon it. In Figure 4a, example cases of nonequilibrium flow speeds downwind of a transition from  $z_{0,out}$  to  $z_{0,in}$  are shown. The trajectories highlight that equilibrium depends uniquely on the local roughness, but the approach depends on both roughness values (Equation 3). By Equation 5, convergence of sediment causes deposition, meaning that in a unidirectional wind regime, a decrease (increase) in flux with distance downwind causes aggradation (degradation) in the dune field. Plotting the deposition rate a fixed distance from the roughness transition (here the streamwise length of White Sands dune field,  $S_{ws}$ ) for different pairs of roughness lengths illustrates that for domains rougher inside than outside, deposition occurs inside because flow is decelerating (Figure 4b). For the pair of roughness lengths assumed for White Sands, the predicted aggradation rate agrees with optically stimulated luminescence (OSL) dating by Kocurek et al. (2007) of 0.5 mm/yr, when the flux intermittency factor (0.05) is chosen so the upwind flux matches Figure 2. The distance downwind  $S_{sat}$  needed to achieve equilibrium between  $z_{0,in}$  and  $U_{10}$  is defined graphically as the distance  $S_d$  such that  $U_{10}$  is first within 1% of  $U_{sat}$  (gray bands in Figure 4a). This lengthscale is shown for roughness length pairs in Figure 4c, with  $S_{sat}$  for White Sands (32 km, red dot) far exceeding  $S_{ws}$  (5 km, yellow line), implying that flow across the entire White Sands dune field is out of equilibrium.

#### 4. Discussion

Our interpretation of the White Sands results is that the majority of the downwind decrease in sediment flux, and associated dune migration rate, can be related to the roughness transition at the dune field boundary. While these dynamics were anticipated by Jerolmack et al. (2012), our work provides (i) the first direct wind measurements demonstrating flow adjustment; (ii) application of a more physically informed model; and (iii) an improved treatment of sand flux. We suspect that the flow disequilibrium extends well beyond the dune field at White Sands, as indicated by the theoretical results ( $S_{ws} \ll S_{sat}$ ) and the observed aggradation across the entire dune field (Figure 2). We also expect that the observed downwind gradients in vegetation density, grain size, dune morphology, and water table depth at White Sands (Ewing & Kocurek, 2010; Jerolmack et al., 2012; Lee et al., 2019) would all be dramatically different if the upwind conditions were altered.

Limitations exist on the application and interpretation of this work. The influence of roughness transitions on flow can be outweighed by other land-ABL interactions, notably the exchange of heat can dominate ABL flow profiles on short time scales (Stull, 2012). Indeed, at White Sands flow profiles are extremely sensitive to the diurnal cycle (Frank & Kocurek, 1994; Gunn et al., 2018); however, we expect the spatial imprint of

these properties during sediment transport to be small relative to that of the roughness. Flow direction and the dune field boundary are clear at White Sands, but other cases are less conducive to this form of analysis. Some dunes, such as giant and isolated star dunes or compound dunes, likely fail to behave as roughness elements in the flow and therefore fall outside the constraints of this analysis. Finally, flow that is out of equilibrium with the surface outside a dune field will not behave as outlined here as it evolves over the dunes. This case probably exists for some dune fields; however, we are confident that Equation 3 applies at White Sands, and the observations of flow deceleration and profile alteration are robust.

More generally, this macroscopic lengthscale of flow and form disequilibrium,  $S_{sat}$ , can be considered alongside other fundamental lengths in aeolian landscape evolution and is similar to  $L_{sat}$ , the saturation length of saltation that sets the dune instability wavelength (Durán et al., 2011).  $S_{sat}$  can be considered the minimum length a dune field must be to attain equilibrium with the ABL. An important distinction, however, is that  $S_{sat}$  depends on conditions outside the dune field as well as those within (highlighted by the diagonal asymmetry in Figure 4c). Dune interaction and migration within  $S_{sat}$  of the dune field windward edge is fundamentally different from when the ABL is equilibrated with the macroscopic dune roughness. Based on the relative length of  $S_{sat}$  values (Figure 4c) and typical dune field lengths ( $10^1$  to  $10^3$  km), we hypothesize that a significant portion of Earth's dunes exist within this out-of-equilibrium edge of dune fields (also suggested by Gao et al., 2015).

Interestingly, the theory suggests that the flux and wind vector directions also change alongside their length inside  $S_{sat}$  due to the evolving importance of drag relative to geostrophy (Figure S5). White Sands does not have sufficient streamwise extent to observe this effect (a  $22^\circ$  deflection at equilibrium  $S_{sat} = 32$  km, in theory); however, in larger domains the dune direction may be affected (suggested by Warren, 1976). All else equal, deflection would increase with latitude, akin to other large Rossby-number-dependent geomorphic forms like turbidity current channels (Wells & Cossu, 2013). Another untested indication from this theory lies in the evolution of incipient dune fields where the coupling between  $z_{0,in}$  and  $q_s$  is most sensitive. As dunes develop, a dune field may switch from net erosion to deposition if its roughness crosses the external roughness (right to left in Figure 4b). Future tests of this idea could extend to the relative effects of heat flux and roughness transitions at coastal dune fields, or where the surface upwind of a unidirectional dune field has coarse spanwise heterogeneity.

## Data Availability Statements

Codes to reproduce this paper and wind data are in this site (<https://github.com/algunn/dune-impinge>). Topography data are hosted by OpenTopography (<https://opentopo.sdsc.edu/datasets?search=white%20sands>).

## References

- Anderson, W., Passalacqua, P., Porté-Agel, F., & Meneveau, C. (2012). Large-eddy simulation of atmospheric boundary-layer flow over fluvial-like landscapes using a dynamic roughness model. *Boundary-layer meteorology*, 144(2), 263–286.
- Bacik, K. A., Lovett, S., Colm-cille, P. C., & Vriend, N. M. (2020). Wake induced long range repulsion of aqueous dunes. *Physical Review Letters*, 124(5), 054,501.
- Bagnold, R. A. (1941). *The physics of blown sand and desert dunes*. London: Methuen.
- Baitis, E., Kocurek, G., Smith, V., Mohrig, D., Ewing, R. C., & Peyret, A.-P. B. (2014). Definition and origin of the dune-field pattern at white sands, new mexico. *Aeolian Research*, 15, 269–287.
- Barlow, J. F. (2014). Progress in observing and modelling the urban boundary layer. *Urban Climate*, 10, 216–240.
- Bauer, B. O. (1991). Aeolian decoupling of beach sediments. *Annals of the Association of American Geographers*, 81(2), 290–303.
- Bou-Zeid, E., Meneveau, C., & Parlange, M. B. (2004). Large-eddy simulation of neutral atmospheric boundary layer flow over heterogeneous surfaces: Blending height and effective surface roughness. *Water Resources Research*, 40, W02505. <https://doi.org/10.1029/2003WR002475>
- Bristow, N. R., Blois, G., Best, J. L., & Christensen, K. T. (2019). Spatial scales of turbulent flow structures associated with interacting barchan dunes. *Journal of Geophysical Research: Earth Surface*, 124, 1175–1200. <https://doi.org/10.1029/2018JF004981>
- Dupont, S., & Brunet, Y. (2009). Coherent structures in canopy edge flow: A large-eddy simulation study. *Journal of Fluid Mechanics*, 630, 93–128.
- Durán, O., Claudin, P., & Andreotti, B. (2011). On aeolian transport: Grain-scale interactions, dynamical mechanisms and scaling laws. *Aeolian Research*, 3(3), 243–270.
- Eastwood, E. N., Kocurek, G., Mohrig, D., & Swanson, T. (2012). Methodology for reconstructing wind direction, wind speed and duration of wind events from aeolian cross-strata. *Journal of Geophysical Research*, 117, F03035. <https://doi.org/10.1029/2012JF002368>
- Ewing, R. C., & Kocurek, G. A. (2010). Aeolian dune interactions and dune-field pattern formation: White sands dune field, new mexico. *Sedimentology*, 57(5), 1199–1219.
- Frank, A., & Kocurek, G. (1994). Effects of atmospheric conditions on wind profiles and aeolian sand transport with an example from white sands national monument. *Earth Surface Processes and Landforms*, 19(8), 735–745.

## Acknowledgments

We are very grateful for David Bustos's continuing facilitation of research at White Sands National Monument. We thank Scott R. David and Kieran B.J. Dunne for field assistance, Elie Bou-Zeid for useful discussions, and Gary Kocurek for topography data (D.O.Is. 10.5069/G9ZK5DMD and 10.5069/G9Q23X5P). Funding provided by National Science Foundation (NSF) NRI INT Award 1734355 to D. J. J.; White Sands National Monument through NPS-GC-CESU Cooperative Agreement P12AC51051 and NSF through the National Center for Airborne Laser Mapping's EAR Award 1043051 for topography data (D.O.I. 10.5069/G97D2S2D) to R. C. E.; International Society of Aeolian Research through the Elsevier Aeolian Research Scholarship to A. G.; and UPenn Earth and Environmental Science department in support of the GEOL305 class. We thank Travis Swanson and Will Anderson for their thought-provoking and conscientious reviews.

- Gao, X., Narteau, C., & Rozier, O. (2015). Development and steady states of transverse dunes: A numerical analysis of dune pattern coarsening and giant dunes. *Journal of Geophysical Research: Earth Surface*, 120, 2200–2219. <https://doi.org/10.1002/2015JF003549>
- Garratt, J. R. (1990). The internal boundary layer a review. *Boundary-Layer Meteorology*, 50(1–4), 171–203.
- Garratt, J. R. (1994). *The atmospheric boundary layer*. Cambridge: Cambridge University Press.
- Ghisalberti, M. (2009). Obstructed shear flows: Similarities across systems and scales. *Journal of Fluid Mechanics*, 641, 51.
- Gunn, A., Wanker, M., Lancaster, N., Edmonds, D. A., Ewing, R. C., & Jerolmack, D. J. (2018). Circadian rhythm of dune-field activity. arXiv preprint arXiv:1812.03612.
- Herrmann, M. J., & Madsen, O. S. (2007). Effect of stratification due to suspended sand on velocity and concentration distribution in unidirectional flows. *Journal of Geophysical Research*, 112, C02006. <https://doi.org/10.1029/2006JC003569>
- Hinds, B. D., & Hoidale, G. B. (1977). *Boundary layer dust occurrence iv atmospheric dust over selected geographical areas*. White Sands Missile Range, New Mexico: Army Electronics Command, Atmospheric Sciences Lab.
- Ho, T. D., Valance, A., Dupont, P., & El Moutar, A. O. (2011). Scaling laws in aeolian sand transport. *Physical Review Letters*, 106(9), 094,501.
- Jerolmack, D. J., Ewing, R. C., Falcini, F., Martin, R. L., Masteller, C., Phillips, C., et al. (2012). Internal boundary layer model for the evolution of desert dune fields. *Nature Geoscience*, 5(3), 206–209.
- Jerolmack, D. J., Mohrig, D., Grotzinger, J. P., Fike, D. A., & Watters, W. A. (2006). Spatial grain size sorting in eolian ripples and estimation of wind conditions on planetary surfaces: Application to meridiani planum, mars. *Journal of Geophysical Research*, 111, E12S02. <https://doi.org/10.1029/2005JE002544>
- Jerolmack, D. J., Reitz, M. D., & Martin, R. L. (2011). Sorting out abrasion in a gypsum dune field. *Journal of Geophysical Research*, 116, F02003. <https://doi.org/10.1029/2010JF001821>
- Kocurek, G., Carr, M., Ewing, R., Havholm, K. G., Nagar, Y. C., & Singhvi, A. K. (2007). White sands dune field, new mexico: Age, dune dynamics and recent accumulations. *Sedimentary Geology*, 197(3–4), 313–331.
- Kocurek, G., & Ewing, R. C. (2005). Aeolian dune field self-organization—implications for the formation of simple versus complex dune-field patterns. *Geomorphology*, 72(1–4), 94–105.
- Kok, J. F., Parteli, E. ricJ. R., Michaels, T. I., & Karam, D. B. (2012). The physics of wind-blown sand and dust. *Reports on Progress in Physics*, 75(10), 106901.
- Lee, D. B., Ferdowsi, B., & Jerolmack, D. J. (2019). The imprint of vegetation on desert dune dynamics. *Geophysical Research Letters*, 46, 12,041–12,048. <https://doi.org/10.1029/2019GL084177>
- Lentz, S. J. (2001). The influence of stratification on the wind-driven cross-shelf circulation over the north carolina shelf. *Journal of Physical Oceanography*, 31(9), 2749–2760.
- Li, B., Sherman, D. J., Farrell, E. J., & Ellis, J. T. (2010). Variability of the apparent von kármán parameter during aeolian saltation. *Geophysical Research Letters*, 37, L15404. <https://doi.org/10.1029/2010GL044068>
- Martin, R. L., Barchyn, T. E., Hugenholtz, C. H., & Jerolmack, D. J. (2013). Timescale dependence of aeolian sand flux observations under atmospheric turbulence. *Journal of Geophysical Research: Atmospheres*, 118, 9078–9092. <https://doi.org/10.1002/jgrd.50687>
- McKee, E. D. (1966). Structures of dunes at white sands national monument, new mexico (and a comparison with structures of dunes from other selected areas). *Sedimentology*, 7(1), 3–69.
- Momen, M., & Bou-Zeid, E. (2016). Large-eddy simulations and damped-oscillator models of the unsteady ekman boundary layer. *Journal of the Atmospheric Sciences*, 73(1), 25–40.
- Momen, M., & Bou-Zeid, E. (2017). Analytical reduced models for the non-stationary diabatic atmospheric boundary layer. *Boundary-Layer Meteorology*, 164(3), 383–399.
- Nield, J. M., King, J., Wiggs, G. F. S., Leyland, J., Bryant, R. G., Chiverrell, R. C., et al. (2013). Estimating aerodynamic roughness over complex surface terrain. *Journal of Geophysical Research: Atmospheres*, 118, 12,948–12,961. <https://doi.org/10.1002/2013JD020632>
- Nikuradse, J. (1950). *Laws of flow in rough pipes*. Washington, DC: National Advisory Committee for Aeronautics.
- Pedersen, A., Kocurek, G., Mohrig, D., & Smith, V. (2015). Dune deformation in a multi-directional wind regime: White sands dune field, new mexico. *Earth Surface Processes and Landforms*, 40(7), 925–941.
- Pelletier, J. D. (2015). Controls on the large-scale spatial variations of dune field properties in the barchanoid portion of white sands dune field, new mexico. *Journal of Geophysical Research: Earth Surface*, 120, 453–473. <https://doi.org/10.1002/2014JF003314>
- Pye, K., & Tsoar, H. (2008). *Aeolian sand and sand dunes*. London: Springer Science & Business Media.
- Reitz, M. D., Jerolmack, D. J., Ewing, R. C., & Martin, R. L. (2010). Barchan-parabolic dune pattern transition from vegetation stability threshold. *Geophysical Research Letters*, 37, L19402. <https://doi.org/10.1029/2010GL044957>
- Shockling, M. A., Allen, J. J., & Smits, A. J. (2006). Roughness effects in turbulent pipe flow. *Journal of Fluid Mechanics*, 564, 267.
- Stevens, R. J. A. M., Gayme, D. F., & Meneveau, C. (2015). Coupled wake boundary layer model of wind-farms. *Journal of Renewable and Sustainable Energy*, 7(2), 023,115.
- Stull, R. B. (2012). *An introduction to boundary layer meteorology* (Vol. 13). London: Springer Science & Business Media.
- Swanson, T., Mohrig, D., & Kocurek, G. (2016). Aeolian dune sediment flux variability over an annual cycle of wind. *Sedimentology*, 63(6), 1753–1764.
- Wang, C., & Anderson, W. (2019). Turbulence coherence within canonical and realistic aeolian dune-field roughness sublayers. *Boundary-Layer Meteorology*, 173(3), 409–434.
- Warren, A. (1976). Dune trend and the ekman spiral. *Nature*, 259(5545), 653–654.
- Wells, M., & Cossu, R. (2013). The possible role of coriolis forces in structuring large-scale sinuous patterns of submarine channel-levee systems. *Philosophical Transactions of the Royal Society A: Mathematical, Physical and Engineering Sciences*, 371(2004), 20120366.